Single-Crystalline Ferromagnetic $Fe_{1-x}Co_xSi$ Nanowires

Juneho In,[†] Kumar S. K. Varadwaj,[†] Kwanyong Seo,[†] Sunghun Lee,[†] Younghun Jo,[‡] Myung-Hwa Jung,[‡] Jinhee Kim,[§] and Bongsoo Kim*,[†]

Department of Chemistry, KAIST, Daejeon 305-701, Korea, Quantum Material Research Team, KBSI, Daejeon 305-333, Korea, and Leading-Edge Technology Group, KRISS, Daejeon 305-600, Korea

Received: November 1, 2007; In Final Form: December 17, 2007

We report the synthesis of ternary $Fe_{1-x}Co_xSi$ nanowires by a vapor transport method. Structural characterization of the nanowires shows a single-crystalline nature with B20 crystal structure. Spatially resolved elemental analysis revealed the homogeneous distribution of all elemental components along the nanowire. The nanowire ensemble shows ferromagnetic properties with a sudden change in magnetization at applied magnetic field near zero. Magnetoresistance measurements on a single-nanowire device show positive magnetoresistance, which does not saturate up to the highest applied field. These ferromagnetic nanowires could find application as spin filters in the new field of nanospintronics.

Introduction

One-dimensional single-crystalline magnetic nanowires (NWs) have been attracting much interest because of their potential applications as key parts in spintronic devices.[1] The magnetic NWs may provide high carrier concentrations and efficient spin-injection because of the radial confinement of carriers and could also be used as spin filters to supply spin-polarized currents. In addition, they could have large magnetic anisotropy energies.[2] Therefore, controlled synthesis of single-crystalline magnetic NWs and fundamental understanding of their properties would be highly valuable for the realization of spintronic devices.

Among the magnetic transition metal silicides, the $Fe_{1-x}Co_xSi$ dilution series has drawn special attention for its interesting electromagnetic characteristics. Simple partial chemical substitution of Co into FeSi not only achieved half metallicity, low-to-intermediate carrier density, and strong spin−orbit coupling, which are desirable in spintronic materials, but also led to unusual positive magnetoresistance and helical spin order.[3] This transition metal silicide also showed a large anomalous Hall effect, comparable in magnitude to dilute magnetic semiconductors (DMS), and it would have the advantage of long spin coherence lifetimes because of the spin-zero ^{28}Si isotopes.[4,5] All these observations suggest great possibilities for $Fe_{1-x}Co_xSi$ NWs in spintronics applications and urged us to synthesize and explore their interesting properties in the nanodimension.

Herein we report the synthesis of freestanding single-crystalline $Fe_{0.9}Co_{0.1}Si$ NWs. The magnetic measurements show ferromagnetic properties in the NW ensemble below Curie temperature (T_C) close to 38 K. The MR measurements from the single NW device show positive MR in all temperatures below T_C. These results, agreeing well with those observed in bulk single-crystalline samples, as well as the energy dispersive X-ray spectroscopy (EDS) mapping show the high quality and homogeneous nature of the NWs.

The synthesis and property measurements on transition metal silicide NWs were extensively investigated recently for their potential use as interconnects and ohmic contacts to complementary metal-oxide semiconductor (CMOS) transistors.[6] It has already been realized that $FeCl_3$ and $CoCl_2$ precursors react with a Si substrate at high temperature to form free-standing FeSi and CoSi NWs.[7] We further developed the synthetic process to selectively produce Fe_5Si_3 and Co_2Si NWs by directly growing the NWs from the vapor phase on sapphire substrate.[8] This is the first report on synthesis of single-crystalline ternary silicide NWs. The composition of $Fe_{0.9}Co_{0.1}Si$ NWs is uniform along the length of the NW, and different NWs show a very narrow composition distribution.

Experimental Section

Single-crystalline $Fe_{1-x}Co_xSi$ NWs were synthesized by use of a 1-in. diameter quartz tube in a horizontal hot-wall two-zone furnace as shown in Scheme 1. The temperatures of the two zones were independently controlled. Precursors were vaporized in an upstream heating zone (A) and the NW grew on the Si substrate in a downstream heating zone (B). Anhydrous FeI_2 powder (0.05 g, 99.99%, Sigma−Aldrich) and CoI_2 powder (0.05 g, 99.99%, Sigma−Aldrich) were used as iron and cobalt precursors, respectively, and placed in a small alumina boat. The carrier argon gas was supplied through a mass flow controller at the rate of 150∼200 sccm. A Si substrate was placed at approximately 12 cm (*d* value in Scheme 1) downstream from the location of a precursor and became the source of Si for silicide formation. Temperatures of heating zones A and B were maintained at 500 and 900 °C, respectively, for 15 min of reaction time at atmospheric pressure condition. No catalyst was used for the NW synthesis.

X-ray diffraction (XRD) patterns of the specimen were recorded on a Rigaku D/max-rc (12 kW) diffractometer operated at 40 kV and 80 mA with filtered 0.154 05 nm Cu Kα radiation. Field emission scanning electron microscope (FESEM) images of $Fe_{1-x}Co_xSi$ NWs were taken on a Phillips XL30S. Transmission electron microscope (TEM) and high-resolution TEM (HRTEM) images and selected area electron diffraction (SAED) patterns were taken on a JEOL JEM-2100F transmission electron microscope operated at 200 kV. After nanostructures were

* Corresponding author: e-mail bongsoo@kaist.ac.kr.
[†] KAIST.
[‡] KBSI.
[§] KRISS.

10.1021/jp7105346 CCC: $40.75
Published on Web 03/01/2008

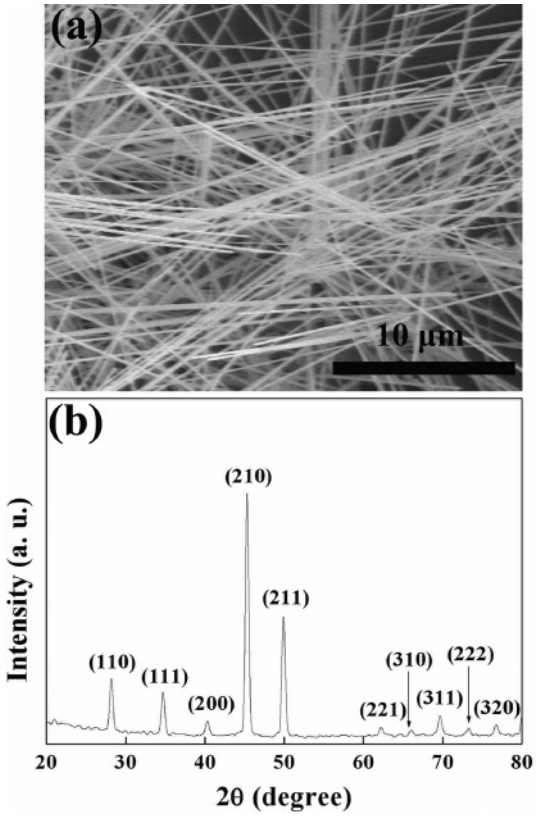

Figure 1. (a) SEM image of $Fe_{1-x}Co_xSi$ NWs. (b) XRD pattern of as-grown $Fe_{1-x}Co_xSi$ NWs.

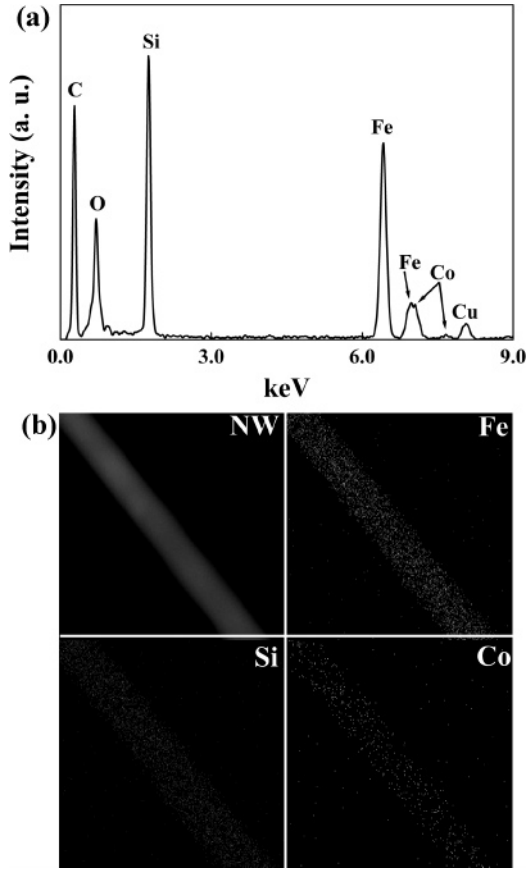

Figure 2. TEM−EDS analysis of single $Fe_{1-x}Co_xSi$ NW: (a) EDS spectrum from the center of the $Fe_{1-x}Co_xSi$ NW; (b) EDS mapping for each element.

dispersed in ethanol, a drop of the solution was put on the holey carbon coated copper grid in preparation for TEM analysis.

Results and Discussion

The morphology of the NWs was examined by FESEM and TEM. A representative SEM image at low magnification in Figure 1a shows NWs in high density on the substrate. The NWs are tens of micrometers long and 60−100 nm in diameter. Figure 1b shows the XRD pattern from the as-grown NW ensemble, in which all the diffraction peaks are indexed to the standard FeSi with a cubic B20 structure (JCPDS file 38-1977). FeSi, CoSi, and all the solid solution series among them ($Fe_{1-x}Co_xSi$) have the same B20 crystal structure with the lattice constant being linearly dependent on Co concentration. Because of the large XRD peak widths of the as-prepared NW sample, the concentration of Co in the NWs could not be determined from the shift in the peak positions.

Therefore, to further understand the chemical composition and elemental distribution in the NWs, an extensive EDS study was performed on various NWs. The EDS spectrum in Figure 2a from a single NW shows that Fe, Co, and Si are the only elements present in the NW (the peaks for C and Cu are from the TEM grid). The EDS spectra from various NWs show that the atomic percentages of Co and Fe are approximately 5% and 45%, respectively, under our reaction conditions. The elemental mapping for a single NW (as shown in Figure 2b) further shows homogeneous distribution of Fe, Co, and Si within the NW lattice. HRTEM and electron diffraction (ED) analysis was used to characterize the structure of the NWs. Figure 3a shows the TEM image and SAED pattern obtained from a representative $Fe_{1-x}Co_xSi$ NW. The SAED pattern of the NW shows a regular spot pattern, indicating the single-crystalline nature of the NWs. The diffraction pattern can be fully indexed to the cubic B20 structure and shows that the NW has [110] growth direction. Figure 3b shows the HRTEM image of a NW with clear lattice fringes. The lattice spacing of the planes perpendicular to the

SCHEME 1: Experimental Set-up

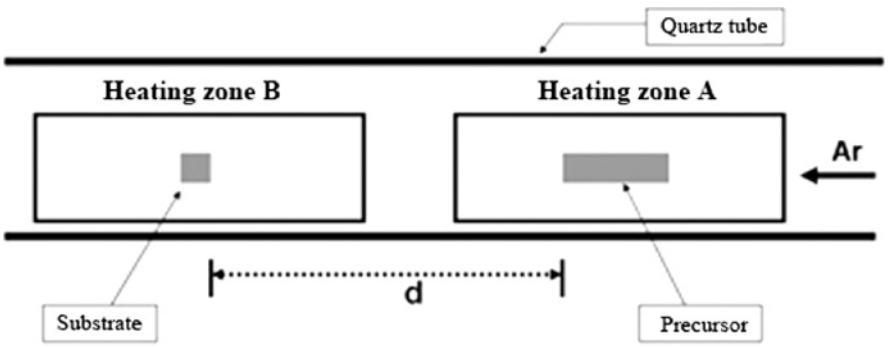

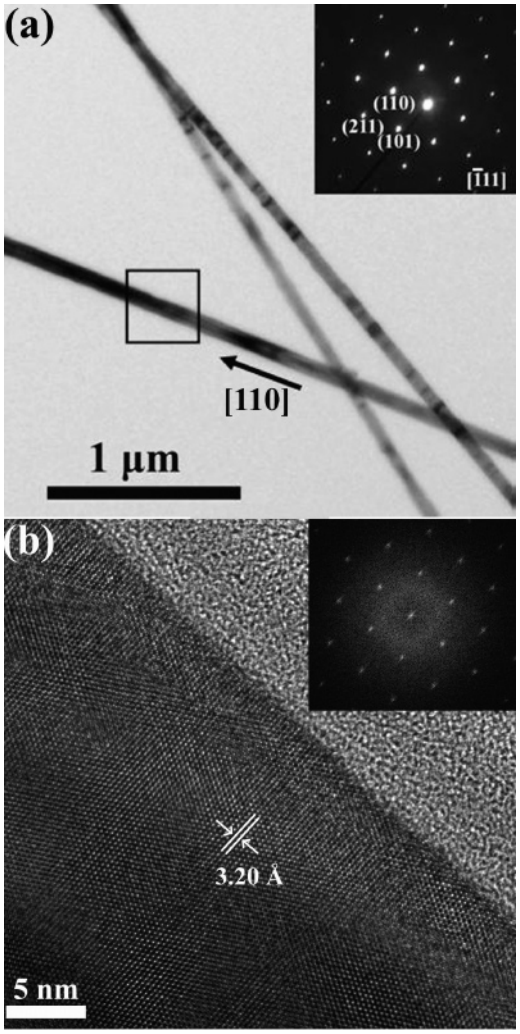

Figure 3. (a) TEM image and (inset) SAED pattern of $Fe_{1-x}Co_xSi$ NW. The SAED pattern is indexed for a cubic $Fe_{1-x}Co_xSi$ NW down the [$\bar{1}$11] zone axis, and the arrow shows the [110] growth direction. (b) HRTEM image shows lattice spacing of 0.32 nm corresponding to the interplanar (110) distance of cubic B20 structure. (Inset) Two-dimensional fast Fourier transform (FFT) from the HRTEM.

growth direction is calculated to be 0.32 nm, which agrees well with the spacing of the (110) planes of cubic FeSi. The two-dimensional fast Fourier transform (FFT) of the lattice resolved image (inset of Figure 3b) obtained from the HRTEM can also be indexed to the cubic B20 structure.

Because no catalytic metal particles or thin films are employed in the synthesis, vapor−liquid−solid (VLS) growth is unlikely. SEM and TEM studies also do not show the presence of any metal catalyst on the NW tip. Moreover, detailed EDS studies of various NWs show that the composition of the tips does not show any significant deviation from that of stems. The reaction pathways for the synthesis of FeSi and CoSi NWs on a Si substrate from the respective metal halide precursors were discussed in detail in our previous reports.[7b,8] In these reactions, we have shown that the NWs are formed by the direct reaction of metal halide precursors with a Si substrate at high temperature. We suggest that the formation of $Fe_{1-x}Co_xSi$ NWs on a Si substrate follows a similar reaction path. Either increase of the precursor vapor pressure, by raising the precursor evaporation temperature, or reduction of the reaction pressure produces secondary growth on the NW surface, with further change producing microparticles. The optimum conditions for the NW formation are achieved by adjusting the precursor vapor pressure

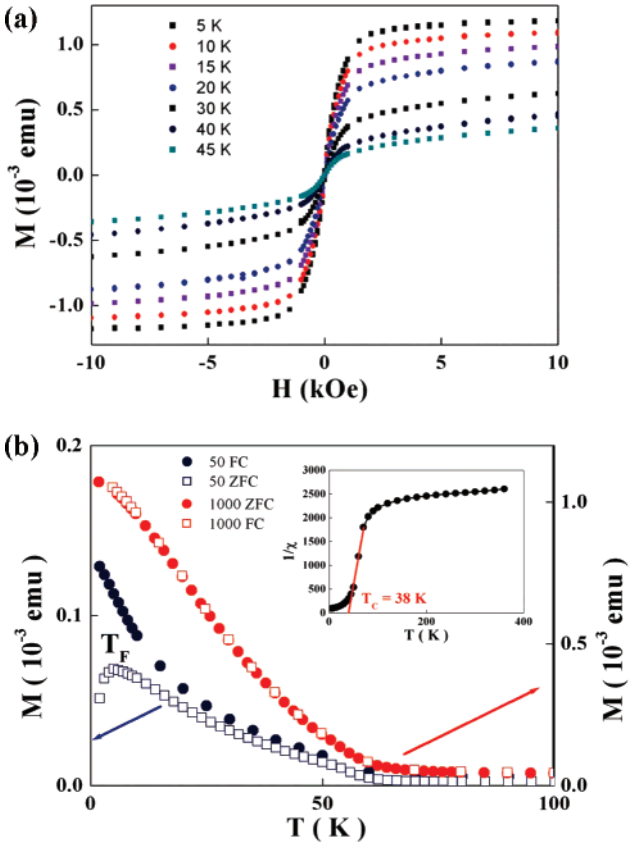

Figure 4. (a) Plot of M as a function of H obtained from the $Fe_{1-x}Co_xSi$ NW ensemble at 5−45 K. (b) Plot of M vs T obtained from $Fe_{1-x}Co_xSi$ NW ensemble at applied fields of 50 and 1000 Oe. Open squares and solid circles represent the ZFC and FC data, respectively. The freezing temperature T_F is marked in the ZFC curve at applied field of 50 Oe. (Inset) Extrapolation of inverse susceptibility ($1/\chi$) plot.

and the substrate temperature. The choice of the appropriate halide precursors and their mixing ratio is most critical to the high-density production of NWs in which Fe and Co are uniformly distributed. The maximum concentration of Co in the NW is 7%, which was obtained when FeI_2 and CoI_2 were taken in a 1:1 atomic ratio. Addition of more CoI_2 in the precursor mixture to increase the Co concentration did not produce $Fe_{1-x}Co_xSi$ NWs with good morphology. Further studies are underway to systematically change the Co concentration in the family of alloy $Fe_{1-x}Co_xSi$ NWs by using various combinations of precursors.

The magnetic properties of as-grown $Fe_{1-x}Co_xSi$ NW ensemble were studied by superconducting quantum interference device (SQUID) magnetometry. Figure 4a shows the plot of sample magnetization M, measured as a function of an applied magnetic field H at various temperatures. At 5 K, the magnetization becomes saturated abruptly for $H > 0$ and $H < 0$. This behavior was previously observed in ferromagnets with helical spin order, such as bulk $Fe_{1-x}Co_xSi$ and MnSi, due to the easy alignment of the helical spins in the magnetization direction.[9,10] The helical spin order in these materials is due to the Dzyalosinsky−Moriya (DM) interaction, occurring by the lack of inversion symmetry of the cubic B20 structure.[11−13] In the present case, although further investigations are necessary to understand the spin structure in the $Fe_{1-x}Co_xSi$ NWs, when the cubic B20 structure of the crystal lattice (as observed in Figures 1b and 3a) is taken into consideration, the $M-H$ behavior may be attributed to the presence of helimagnetic order in the NWs. Figure 4b shows the temperature-dependent zero-field-cooled (ZFC) and field-cooled (FC) magnetization of the NW ensemble

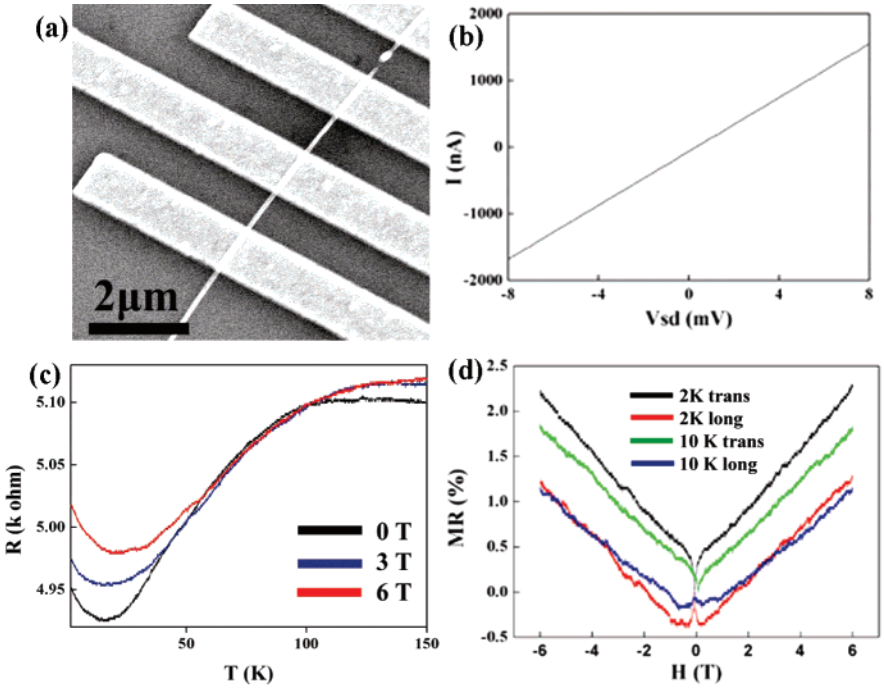

Figure 5. (a) SEM image of the NW device. (b) $I-V$ curve of single $Fe_{1-x}Co_xSi$ NW at 2 K. (c) Temperature-dependent resistance at applied fields of 0 T (black), 3 T (blue), and 6 T (red). (d) Longitudinal and transverse *MR* (%) of single $Fe_{1-x}Co_xSi$ NW at 2 and 10 K.

measured under applied fields of 50 and 1000 Oe, respectively. At low H and low T, two distinct features are observed in the FC and ZFC curves. The ZFC curve measured at an applied field of 50 Oe shows a peak at $T_F = 5$ K, and a distinctive divergence of FC and ZFC curves is observed with steep increase of FC magnetization at temperatures lower than T_F. The FC and ZFC curves completely merge under applied fields higher than 500 Oe. These features in the magnetic response are also observed in the single-crystalline bulk $Fe_{1-x}Co_xSi$ sample and resemble closely reentrant spin-glass-like behavior.[14] The Curie−Weiss plot ($1/\chi$ vs T) is shown in Figure 4b as an inset, yielding a T_C close to 38 K. This value is consistent with single-crystal bulk samples in which the value of Co doping is $x = 0.15$ ($T_C = 25$ K) and $x = 0.2$ ($T_C = 35$ K).[3a]

Transport studies and magnetoresistance measurements have been carried out on individual $Fe_{1-x}Co_xSi$ NWs. The device for the magnetoresistance measurements was prepared by dispersing the NWs on a SiO_2-coated Si substrate. The position of a single NW was located with reference to predefined marks, and the nanoelectrodes of 20 nm Ti and 80 nm Au were fabricated by a standard electron-beam lithography technique (Supporting Information). Figure 5a shows the SEM image of such a NW device. The electron transport measurements were carried out by the physical property measurement system (PPMS, Quantum design) with two- and four-probe configurations. The NW device shows a linear current versus voltage curve, which confirms an ohmic contact between the NW and electrodes (Figure 5b). Figure 5c shows the temperature-dependent resistance measured under various external magnetic fields for a single $Fe_{1-x}Co_xSi$ NW. It shows that the magnetoresistance (*MR*) is positive for all $T < T_C$ and thus it is not induced by the magnetic critical fluctuations near the Curie temperature. This type of magnetoresistance in ferromagnets is attributed to the quantum interference effect in which the same electrons are responsible for both the magnetic properties and electrical conduction.[3a] At 2 K, however, the *MR* value is around 2% at applied field of 5 T, which is smaller than that observed in bulk.[3a] This difference in *MR* may be attributed to the disordered surface spin in the NW, which may be responsible for the negative contribution to *MR*.[7b] Figure 5d shows the longitudinal and transverse *MR* with respect to the NW axis at 2 and 10 K up to a field of 6 T. Magnetoresistance is defined as $MR = [R(H) - R(0)]/R(0)$, where $R(H)$ and $R(0)$ are the resistance at an applied field and zero field, respectively. When the magnitude of H is increased, *MR* increases almost linearly except at low fields and does not show any sign of saturation up to the highest field. The transverse *MR* shows a cusplike minimum at low H, suggesting that *MR* and magnetization have some correlation at low H, while the magnetization has no effect on *MR* at high H. At low H, the longitudinal *MR* becomes prominently negative at 2 K, probably due to the anomalous magnetoresistance common to ferromagnets. These observations show that *MR* is anisotropic at low field; such dependence of *MR* on the orientation between the magnetization and the current density may be attributed to the strong spin−orbit coupling.[15] However, the similarity of longitudinal and transverse *MR* at high-field suggests that the orbital contribution is a minor contributor to *MR*. These magnetoresistance properties observed for a single $Fe_{1-x}Co_xSi$ NW are in good agreement with those for the single-crystalline bulk counterpart.

Conclusion

We have synthesized high-density single-crystalline $Fe_{1-x}Co_xSi$ NWs by a vapor transport-based method from simple metal halide precursors. The elemental components are uniformly distributed along the free-standing NWs. The NW ensemble shows ferromagnetic properties with reentrant spin-glass-like behavior. Magnetoresistance measurements on single NW devices show positive *MR*, which is independent of the magnetization behavior at high magnetic field. All these properties are consistent with those of the single-crystalline bulk samples. $Fe_{1-x}Co_xSi$ NWs are the first example of a ternary silicide with unique magnetic and magnetoresistance properties in one-dimensional morphology. This material could play an important role in the fundamental study of nanometric magnetic

domain structures as well as potential applications in the field of nanospintronics.

Acknowledgment. We thank KOSEF for support through the NRL (ROA-2007-000-20127-0), the Center for Intelligent NanoBio Materials (R11-2005-008-00000-0), and the Basic Research Program (R01-2005-000-10711-0). SEM and TEM analyses were performed at the Korea Basic Science Institute in Daejeon.

Supporting Information Available: Fabrication process of single NW device. This material is available free of charge via the Internet at http://pubs.acs.org.

References and Notes

(1) (a) Allwood, D. A.; Xiong, G.; Cooke, M. D.; Faulkner, C. C.; Atkinson, D.; Vernier, N.; Cowburn, R. P. *Science* **2002**, *296*, 2003. (b) Yamaguchi, A.; Ono, T.; Nasu, S.; Miyake, K.; Mibu, K.; Shinjo, T. *Phys. Rev. Lett.* **2004**, *92*, 077205. (c) Beach, G. S. D.; Nistor, C.; Knutson, C.; Tsoi, M.; Erskine, J. L. *Nat. Mater.* **2005**, *4*, 741. (d) Liao, Z.-M.; Li, Y.-D.; Xu, J.; Zhang, J.-M.; Xia, K.; Yu, D.-P. *Nano Lett.* **2006**, *6*, 1087.

(2) (a) Choi, H.-J.; Seong, H.-K.; Chang, J.; Lee, K.-I.; Park, Y.-J.; Kim, J.-J.; Lee, S.-K.; He, R.; Kuykendall, T.; Yang, P. *Adv. Mater.* **2005**, *17*, 1351. (b) Xia, Y.; Yang, P.; Sun, Y.; Wu, Y.; Mayers, B.; Gates, B.; Yin, Y.; Kim, F.; Yan, H. *Adv. Mater.* **2003**, *15*, 353.

(3) (a) Manyala, N.; Sidis, Y.; DiTusa, J. F.; Aeppli, G.; Young, D. P.; Fisk, Z. *Nature* **2000**, *404*, 581. (b) Guevara, J.; Vildosola, V.; Milano, J.; Llois, A. M. *Phys. Rev. B* **2004**, *69*, 184422. (c) Uchida, M.; Onose, Y.; Matsui, Y.; Tokura, Y. *Science* **2006**, *311*, 359.

(4) Manyala, N.; Sidis, Y.; DiTusa, J. F.; Aeppli, G.; Young, D. P.; Fisk, Z. *Nat. Mater.* **2004**, *3*, 255.

(5) Erricsson, M. A.; Friesen, M.; Coppersmith, S. N.; Joynt, R.; Klein, L. J.; Slinker, K.; Tahan, C.; Mooney, P. M.; Chu, J. O.; Koester, S. *J. Quantum Inf. Process.* **2004**, *3*, 133.

(6) (a) Wu, Y.; Xiang, J.; Yang, C.; Lu, W.; Lieber, C. M. *Nature* **2004**, *430*, 61. (b) Schmitt, A. L.; Zhu, L.; Schmeisser, D.; Himpsel, F. J.; Jin, S. *J. Phys. Chem. B* **2006**, *110*, 18142. (c) Schmitt, A. L.; Bierman, M. J.; Schmeisser, D.; Himpsel, F. J.; Jin, S. *Nano Lett.* **2006**, *6*, 1617. (d) Chueh, Y.-L.; Ko, M.-T.; Chou, L.-J.; Chen, L.-J.; Wu, C.-S.; Chen, C.-D. *Nano Lett.* **2006**, *6*, 1637. (e) Song, Y.; Schmitt, A. L.; Jin, S. *Nano Lett.* **2007**, *7*, 965. (f) Szczech, J. R.; Schmitt, A. L.; Bierman, M. J.; Jin, S. *Chem. Mater.* **2007**, *19*, 3238. (g) Seo, K.; Varadwaj, K. S. K.; Cha, D.; In, J.; Kim, J.; Park, J.; Kim, B. *J. Phys. Chem. C* **2007**, *111*, 9072.

(7) (a) Ouyang, L.; Thrall, E. S.; Deshmukh, M. M.; Park, H. *Adv. Mater.* **2006**, *18*, 1437. (b) Seo, K.; Varadwaj, K. S. K.; Mohanty, P.; Lee, S.; Jo, Y.; Jung, M.-H.; Kim, B.; Kim, B. *Nano Lett.* **2007**, *7*, 1240.

(8) Varadwaj, K. S. K.; Seo, K.; In, J.; Mohanty, P.; Park, J.; Kim, B. *J. Am. Chem. Soc.* **2007**, 129. 8594.

(9) Beille, J.; Voiron, J.; Roth, M. *Solid State Commun.* **1983**, *47*, 399.

(10) Ishimoto, K.; Yamaguchi, Y.; Suzuki, J.; Arai, M.; Furusaka, M.; Endoh, Y. *Physica B* **1995**, *213*−*214*, 381.

(11) Dzyaloshinski, I. *J. Phys. Chem. Solids* **1958**, *4*, 241.

(12) Moriya, T. *Phys. Rev.* **1960**, *120*, 91.

(13) Bak, P.; Jensen, M. H. *J. Phys. C* **1980**, *31*, L881.

(14) Chattopadhyay, M. K.; Roy, S. B.; Chaudhary, S. *Phys. Rev. B* **2002**, *65*, 132409.

(15) Campbell, I. A.; Fert, A. *Ferromagnetic Materials*, Vol. 3; North Holland: Amsterdam, 1982.